Recibido: 29/05/2022
Aceptado: 06/07/2022

REVISTA DE TELEDETECCIÓN
Asociación Española de Teledetección
(2022) 60, 71-87
ISSN 1133-0953
EISSN 1988-8740
https://doi.org/10.4995/raet.2022.17770

CASO PRÁCTICO

Water area and volume calculation of two reservoirs in Central Cuba using remote sensing methods. A new perspective

Alexey Valero-Jorge[1], Roberto González-De Zayas*[2,3], Anamaris Alcántara-Martín[4], Flor Álvarez-Taboada[5], Felipe Matos-Pupo[1], Oscar Brown-Manrique[6]

[1] *Centro Meteorológico de Ciego de Ávila. Instituto de Meteorología. Avenida de los Deportes S/N. Ciego de Ávila. Cuba.*
[2] *Departamento de Ingeniería Hidráulica, Facultad de Ciencias Técnicas. Universidad de Ciego de Ávila. Carretera a Morón km 9. Ciego de Ávila. Cuba.*
[3] *Centro de Estudios Geomáticos, Ambientales y Marinos. Ejército Nacional, 404. Mexico City. Mexico.*
[4] *Agencia provincial de GEOCUBA. Avenida Las Palmas y Circunvalación Norte. Ciego de Ávila. Cuba.*
[5] *Escuela de Ingeniería Agraria y Forestal. Universidad de León. Avenida de Astorga S/N. Ponferrada. Spain.*
[6] *Centro de Estudios Hidrotécnicos, Facultad de Ciencias Técnicas. Universidad de Ciego de Ávila. Carretera a Morón km 9. Ciego de Ávila. Cuba.*

Abstract: The availability, quality and management of water constitute essential activities of national, regional and local governments and authorities. Historic annual rain (between 1961 and 2020) in Chambas River Basin (Central Cuba) was evaluated. Two remote sensing methods (Normalized Difference Water Index and RADAR images) were used to calculate the variation of water area and volumes of two reservoirs (Chambas II and Cañada Blanca) of Ciego de Ávila Province at end of wet and dry seasons from 2014-2021. The results showed that mean annual rain was 1330.9 ± 287.4 mm and it did not showed any significant tendency at evaluated period. For both reservoirs, mean water areas measured with two methods were 19 % and 8 % smaller than the mean water area reported by authorities for the same period. The static water storage capacity (water volume) of both reservoirs varied (as area) between seasons with the greatest volume in both reservoirs recorded in October of 2017 (30.5 million of m^3 in Chambas II and 45.1 million of m^3 in Cañada Blanca reservoir). Large deviations of water area and volumes occurred during the dry season (lower values) and the wet season of 2017 (influenced by rain associated to of Hurricane Irma) and wet season of 2020 (influenced by rain associated to tropical storm Laura). Calculated area – volume models with significant statistical correlation are another useful tool that could be used to improve water management in terms of accuracy and to increase reliable results in cases where gauge measurements are scarce or not available.

Key words: water, reservoir, remote sensing, management, Cuba.

Cálculo del área y volumen de agua de dos reservorios de Cuba Central usando métodos de sensores remotos. Una nueva perspectiva

Resumen: La disponibilidad, calidad y manejo del agua constituye actividades esenciales de los gobiernos y autoridades regionales y locales. Fue evaluada La lluvia anual histórica (entre 1961 y 2020) de la Cuenca del Río Chambas. Para el cálculo de la variación de las áreas y volúmenes del agua en dos reservorios de la Provincia de Ciego de Ávila al término de las temporadas lluviosa y poco lluviosa entre 2014 y 2021 fueron usados dos métodos de sensores remotos (Índice Normalizado de Diferencia de Agua e imágenes del RADAR). Los resultados mostraron

To cite this article: Valero-Jorge, A., González-De Zayas, R., Alcántara-Martín, A., Álvarez-Taboada, F., Matos-Pupo, F., Brown-Manrique, O. 2022. Water area and volume calculation of two reservoirs in Central Cuba using remote sensing methods. A new perspective. *Revista de Teledetección*, *60*, 71-87. https://doi.org/10.4995/raet.2021.17770

* *Corresponding author: roberto.gz710803@gmail.com*

que la lluvia media anual fue 1330.9±287.4 mm y no mostró tendencia significativa en el período evaluado. Para ambos reservorios, las áreas promedio de agua medidas con los dos métodos fueron 19 % y 8 % menores que el área de agua reportadas por las autoridades para el mismo período. La capacidad estática de almacenamiento de agua (volumen de agua) de los dos reservorios varió (como el área) entre temporadas, con el mayor volumen determinado en ambos reservorios en octubre de 2017 (30.5 millones de m3 en Chambas II y 45.1 millones de m3 en Cañada Blanca). Grandes desviaciones de las áreas y volúmenes del agua ocurrieron durante la temporada poco lluviosa (menores valores) y la temporada lluviosa de 2017 (influenciada por las lluvias asociadas el huracán Irma) y la temporada lluviosa de 2020 (influenciada por la lluvia asociada a la tormenta Laura). Los modelos calculados para la relación área – volumen con una significación estadística son otra herramienta útil que podría ser usada para mejorar el manejo del agua en términos de precisión y el incremento de resultados confiables en casos donde la medición de los niveles de agua son escasos o no están disponibles.

Palabras clave: agua, reservorio, sensores remotos, manejo, Cuba.

1. Introduction

Water is one of most important economic, social and environmental resources of any country. The availability, quality and management of water constitute essential activities of national, regional and local governments and authorities. According to Mulligan et al. (2020) there are more than 38 000 georeferenced water reservoirs around the world, with the greatest number in tropical land areas. Asia has more than 50 % of the georeferenced dams, followed by South America, Europe (16.5%) and North America (16.4%).

The estimation of water area and volume of reservoirs is made by different methods (the most used is area–volume–elevation (AVE) curve), which are, frequently, criticized by many authors due to lack of true and public information to science (Wang et al., 2013), lack of knowledge of parameters (Naba Sayl et al., 2017), costs and time-consuming process (Karran et al., 2016; Naba Sayl et al., 2017).

In recent decades, new tools such as remote sensing have been developed and used to monitor water reservoirs, including information about water area and volume variability (Du et al., 2012; Nandi et al., 2018; Fuentes et al., 2019), sedimentation (Adediji and Ajibade, 2008; Naba Sayl et al., 2017); and trophic condition (Machado and Baptista, 2016; Lopes et al., 2017). Some of the remote sensing methodologies are developing several spectral indexes such as Normalized Difference Water Index (NDWI) which uses the Green band (GREEN) and near-infrared band (NIR) (McFeeter, 1996) and Modified Normalized Difference Water Index (MNDWI), which is a modification of NDWI proposed by Xu (2006), replacing band 4 by band 5 of Landsat 5 TM in McFeeter's index. Other commonly used indexes related with surface water mapping are Normalized Difference Moisture Index (NDMI) (Wilson and Sader, 2002) and Normalized Difference Vegetation Index (NDVI) (Rouse et al., 1973; Aguilar et al., 2012; Escobar-Flores et al., 2019).

Cuba has, due to its configuration (narrow and long island), short and very seasonally variable rivers that flow to the north and south coasts. However, since the 60´s of 20th Century, many water reservoirs were built to capture and store all available waters (Batista Silva, 2016). According to the database of the National Hydraulic Resources Institute (INRH, in Spanish) (2018), there are 242 reservoirs with approximately 9.1×10^9 m^3 of water volume capacity in Cuba. All this water volume is used for basic economic and social activities and the availability of this resource is monitored carefully by water managers.

The use of remote sensing tools (as NDWI index) to monitor water resources in Cuba is not documented. According to Cruz Flores et al. (2020) only few studies have documented the remote sensing and vegetation indexes in Cuba, and most of them have focused on vegetation cover (Morejón et al., 2010; Denis Ávila, 2015; Ponvert-Delisles, 2016; Hernández and Cruz, 2016; Cobos et al., 2016). For this reason, the principal aim of this study is to evaluate the use of two remote sensing tools to monitor water area and volumes

Table 1. Principal characteristics of Cañada Blanca and Chambas II reservoirs (from INRH database),

	Normal Storage		Maximum Storage		Minimum Storage	
Reservoir	Water level (masl)	Vol (millions of m^3)	Water level (masl)	Vol (millions of m^3)	Water level (masl)	Vol (millions of m^3)
Cañada Blanca	84.0	46.5	87.2	67.5	64.2	0.5
Chambas II	84.0	33.3	87.2	56.0	68.50	0.2

of two water reservoirs in Central Cuba, as a new tool to water management in this region.

2. Materials and Methods

2.1. Study zone

Liberación de Florencia reservoir (former Complejo Hidráulico Liberación de Florencia, in Spanish) is formed by two independent reservoirs (Cañada Blanca and Chambas II) (Table 1). These reservoirs are located near the town of Florencia, in Ciego de Ávila province, Central Cuba (Figure 1). Water of both reservoirs is used, principally, for agriculture and as water supply to Florencia and Tamarindo towns (approximately 15 000 people). The reservoirs were built at end of the last century. Both reservoirs are associated to the Chambas River Basin (68.9 km), the second most important basin (333 km^2) in Ciego de Ávila province.

Climate is characterized by two well defined seasons: the dry season (from November to April) with only 20% of annual rain and the wet season (from May to October) with 80% of annual rain. The reservoirs is from around 70 m to 90 m of height above sea level (h.a.s.l) (Figure 2). At right margin of each reservoir there are installed some metallic limnimeters with precision of 1 cm that are read every day. This lecture (in meters, using the height above sea level) is sent to water authority's manager offices and with AVE curve of each reservoir (made before reservoir construction from topography data for watershed area), the data (volume and area) is reported.

2.2. Historic Rain of the Chambas River Basin

To determine historic rain (from 1961 to 2020) in the Chambas River Basin, the database of the

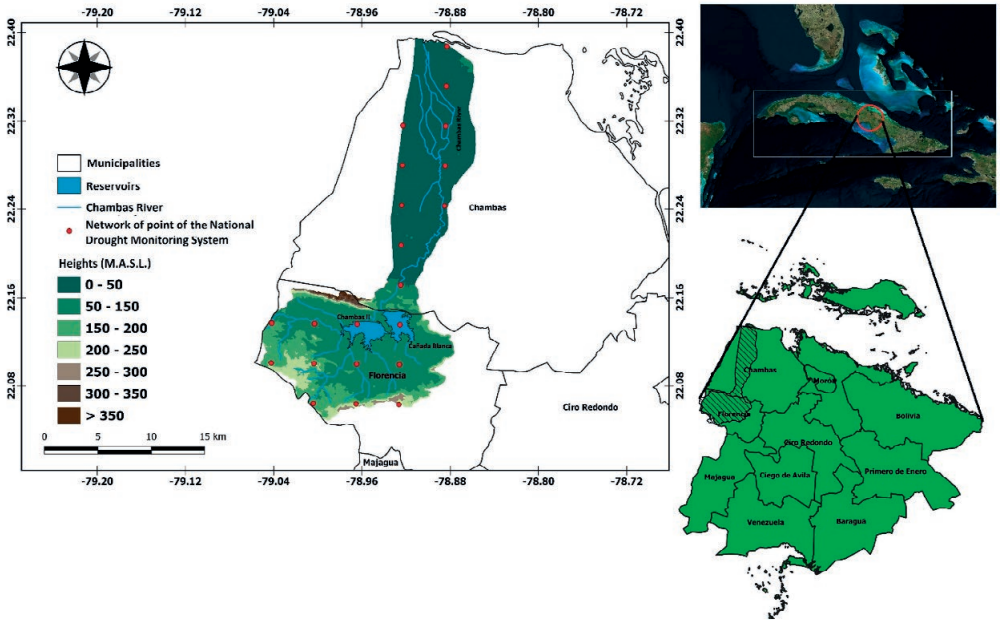

Figure 1. Location of Cañada Blanca and Chambas II reservoirs (Chambas River Basin) in Ciego de Ávila province (Central Cuba).

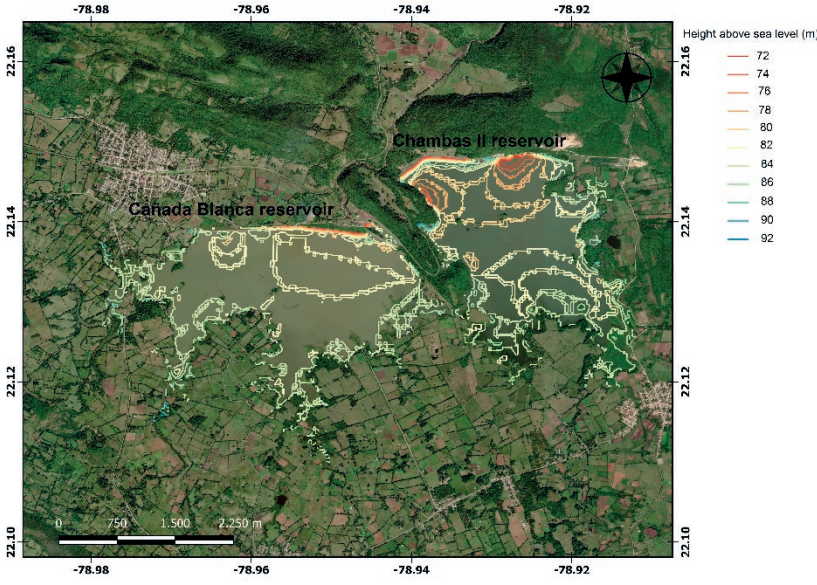

Figure 2. Heights above sea level of two studied reservoirs..

Cuban National Watch Drought System was used. This database has a national network with resolution of 4×4 km and of the national inventory; in Ciego de Ávila province, there are 492 points. For rain analysis in the Chambas River Basin, 21 points inside the basin area were used (Figure 1). This national network was built through interpolation methods from the national network of rain gauge stations, certified and calibrated by the National Institute of Hydraulic Resources of Cuba (for more details, see Valero et al., 2021).

Using the rain database, some maps were made for historic rain distribution in Ciego de Ávila province and for historic rain (dry and wet season) in the Chambas River Basin. All maps were made using software QGIS (version 3.16.11).

2.3. Normalized Difference Water Index (NDWI)

This method (NDWI) uses green (GREEN) and infrared bands (NIR) of spectral images. It is an appropriate tool to map surface waters and inundated areas, due to that water has a high absorption and low irradiation in the visible range of infrared. The NDWI is one ratio methods and is defined as:

Table 2. The NDWI ranges and each description.

Range	Description
0.2–1	Water surface
0.0–0.2	Inundation, humidity
-0.3–0.0	Moderated drought, surface without water
-1–-0.3	Drought, surface without water

The NDWI values can vary between -1 and 1, with the followed ranges (Table 2).

For calculation of NDWI, satellite images Sentinel-2A (10 images of resolution of 10 m) and Landsat 8/OLI (eight images of resolution of 30 m) were downloaded. From these images (Sentinel-2A), only green (B3) and infrared (B8) bands were used, while B3 (green) and B5 (infrared) bands were used for Lansadt 8/OLI. Both images are in the coordinate system WGS 84 and cloud cover was below 20%. The downloaded images were from seven years (from 2014 to 2021) during the same seasons: dry (November–April) and wet (May–October).

The QGIS software (version 3.16.11) was used to process images and to calculate the NDWI. All data were imported to QGIS and then, using the *Raster Calculator* option in main menu, all calculations were implemented to estimating NDWI (Figure 3).

The obtained images with NDWI were reclassified using *Raster Analysis* with ranges of specific values (from -1.0 to 0.19 with value 0 and from 0.2 to 1.0 with value 1), where water areas were separated from the rest of the image areas. This analysis

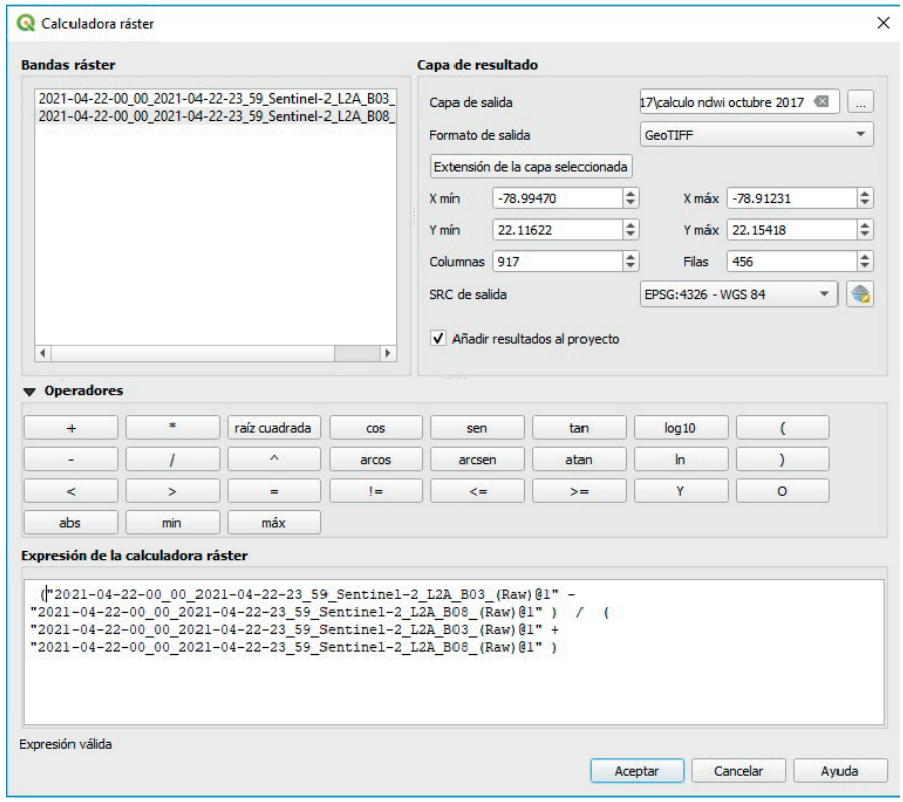

Figure 3. View of process Raster Calculator from QGIS.

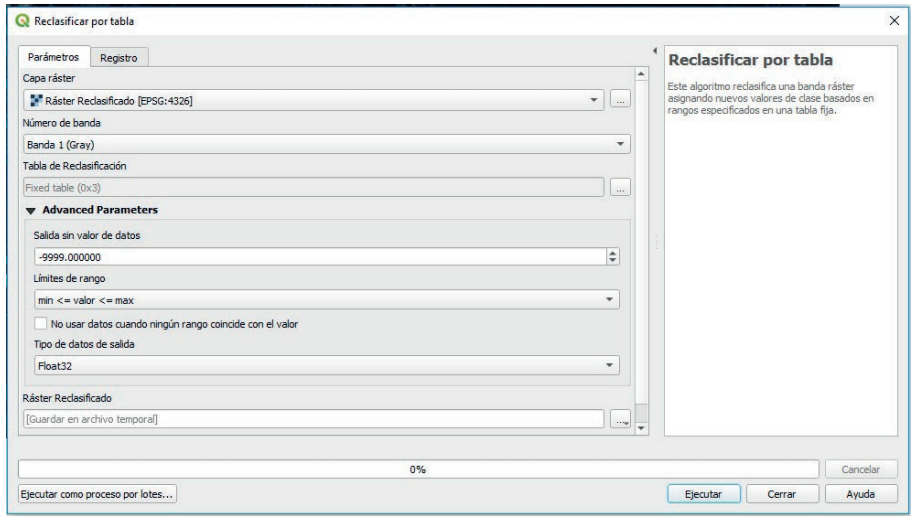

Figure 4. View of process Reclassification by Table

was made using option *Process/Tools Box/Raster analysis/Reclassification by Table* (Figure 4). With this process was obtained a reclassified image by NDWI values (Figure 5).

Once the image was reclassified, water area was calculated using the area that was colored with value 1, using option *r. report* (Figure 6) inside Tools Box of GRASS. Each area was reported in km^2 and the file was saved as a txt file (Figure 7).

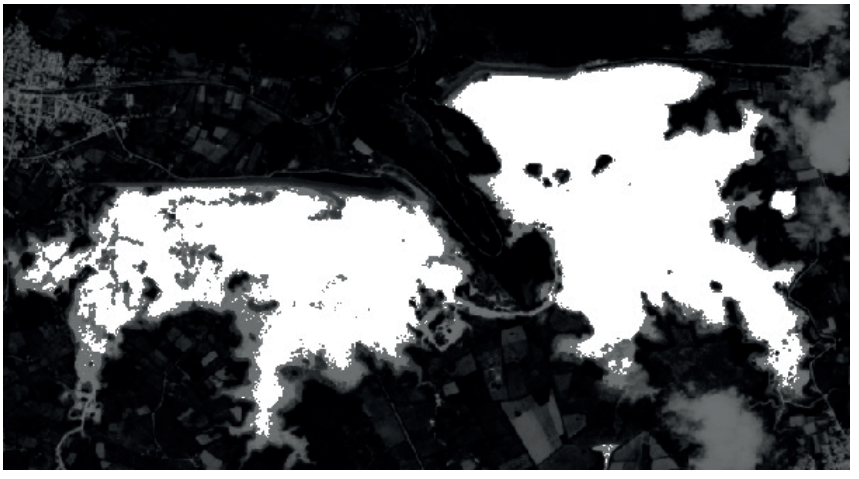

Figure 5. Reclassified image in ranges from NDWI.

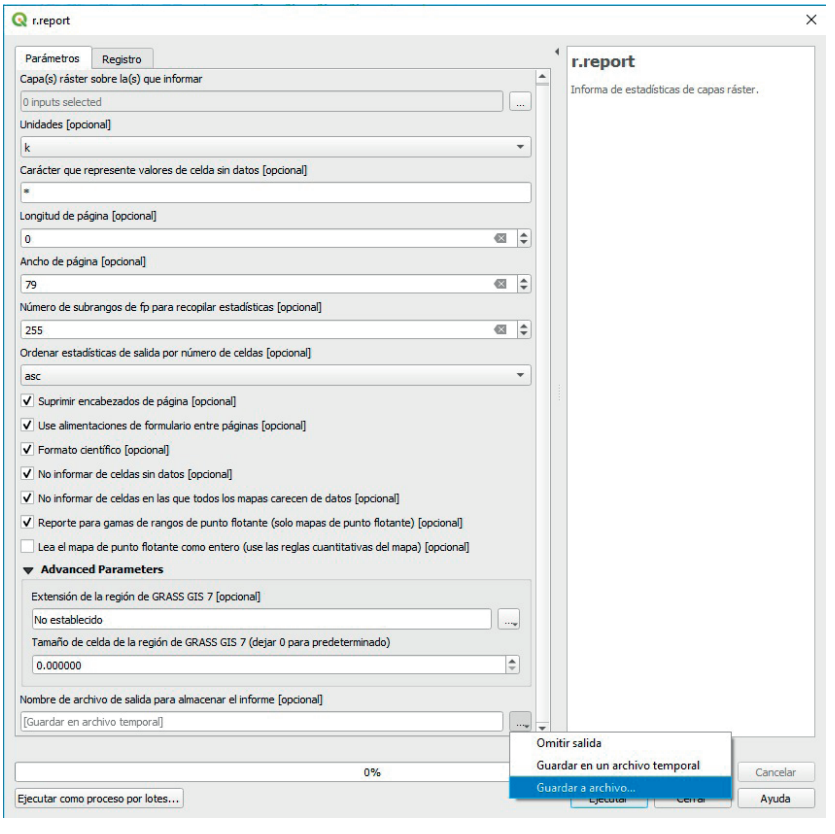

Figure 6. Calculating process for area with *r. report* tool.

2.4. Obtaining and pre-processing of RADAR images of Sentinel-1

Images were downloaded (15) from satellite Sentinel-1A (S1A) using acquisition mode Interpherometric Wide Swath (IW). The downloaded database was of Level 1 GRD (Ground Range Detected), only with multi-looked intensity. These RADAR data were projected with

aa: Bloc de notas

Archivo Edición Formato Ver Ayuda

#	Category Information description	square kilometers
1	. . . . .	6.700312
0	. . . . .	11.554972
-1	. . . . .	50.964396
TOTAL		69.219679

Figure 7. Structure of note archive with report of calculated (in Km^2).

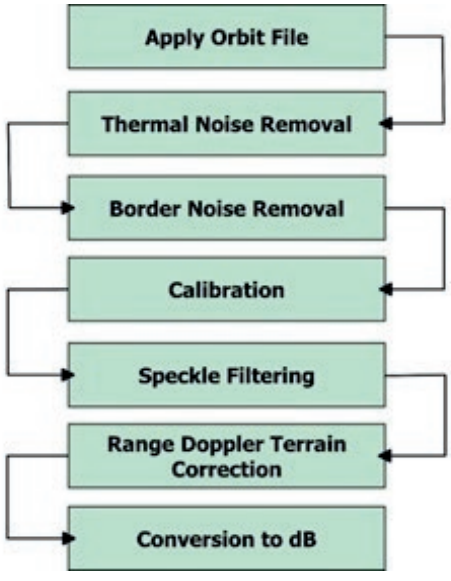

Figure 8. Preprocessing steps applied to images RADAR.

ellipsoidal model WGS-84 and high resolution. Also, double polarometric images (VV-VH) were used, which allows the calculation of polarization of terrain (Muro et al., 2019, 2020; Alarcón, 2021). For better interpretation of images RADAR, a standard preprocessing was made using the steps shown in Figure 8. For preprocessing of images, the software SNAP (Sentinel Application Platform) (version 8.0) was used.

The step Apply Orbit File uses recalculated orbit data, which are necessary to improve the quality of geocodification, and other results of images RADAR processing. When images were perturbed by some thermal noise, particularly at the cross-polarization channel, the Thermal Noise Removal step was used. Border Noise Removal step was applied to diminish some noises at borders of images (Park et al., 2018). The radiometric calibration (Calibration step) is one of the principal processes that assures available values of retro dispersion of pixels in the images. The speckle noises cause many difficulties to read the images correctly; other analysis showed changes in detection and classification of images RADAR, so, the Speckle Filtering steps was used, applying the adaptive filter Lee-Sigma (Lee, 1980, 1981a,b). Using the Range Doppler Terrain Correction step, the geometric distortions (which could provoke errors in geolocalization) were corrected in the last step, bands of retro dispersion were converted to decibels (dB).

For estimating area of reservoirs, the histogram of coefficient of filtered retro dispersion was analyzed (Figure 9). The low values of retro dispersion were for water areas (-18 dB to) (Alarcón, 2021).

For estimating water volumes of reservoir, the QGIS plugin *Volume calculation tools* were used. This algorithm calculates volumes for both, under and above raster surface. This tool has some methods for volume estimating but the *Count above and below (cut/fill)* method was used in this research. For volume calculation using this method, the Digital Elevation Model (DEM) of Ciego de Ávila province was necessary. The DEM of 1:10 000 scale was used; this scale is equivalent to raster image resolution of 5 m of pixel (Jakovljevic et al., 2018).

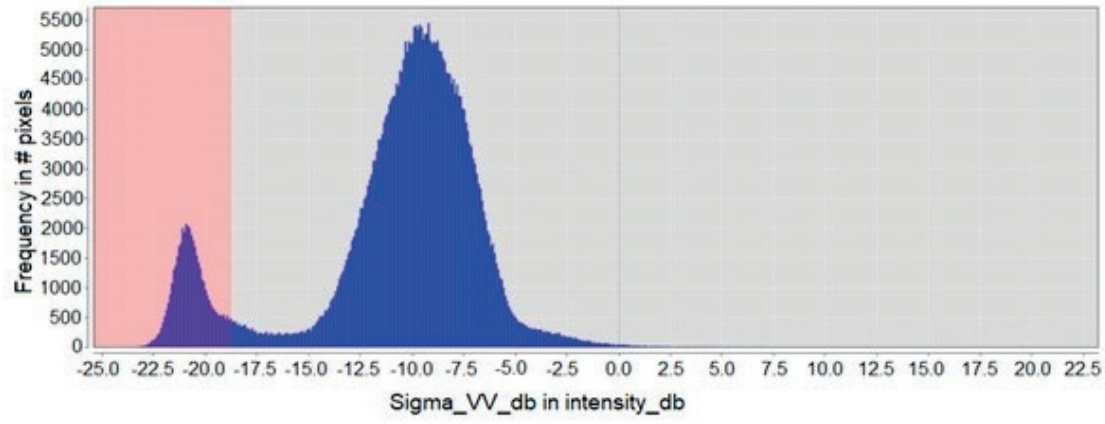

Figure 9. Histogram of coefficient of filtered retro dispersion.

2.5. Statistical analysis

For historic annual rain in the basin, the tendency analysis test was used (Mann-Kendall) (Mann, 1945; Kendall, 1975; Pohlert, 2016). The Non parametric Kruskal-Wallis test was used to find significant differences among water areas and volumes measured with remote sensing methods and those reported by local authorities. Linear regression was applied to find significant correspondence among estimated areas and volumes with the same parameters reported by the National Hydraulic Resources Institute (INRH in Spanish). Same test was applied to find any significant correlation among water areas and volumes of the reservoirs and rain and evaporation for each studied period.

All statistical analyses were made using the XLSTAT software (version 2016.02.28451).

3. Results

3.1. Historic annual rain (1961–2020)

The historic annual rain (from 1961 to 2020) was 1330.9 ± 287.4 mm, with the greatest rain values in 1978 (1965.4 ± 142.1 mm) and 2007 (1874 ± 173.1 mm). The lowest annual rain values were in 1962 (689.3 ± 99.1 mm) and 1965 (693.1 ± 87.4 mm) (Figure 10). Mann-Kendal test did not find any significant tendency in the studied period (1961 – 2020). The same behavior was obtained with the Mann-Kendal test analysis for historic seasonal rain for the dry and wet seasons.

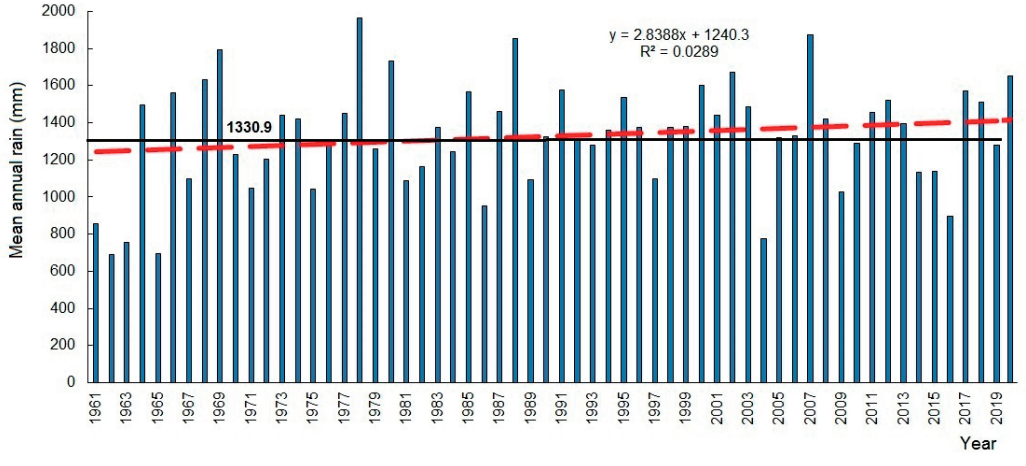

Figure 10. Mean annual rain (1961 – 2020) in Chambas River Basin, Central Cuba. Dotted red line represents tendency (not significant). Black line represents mean rain for the entire period (1330.9 mm).

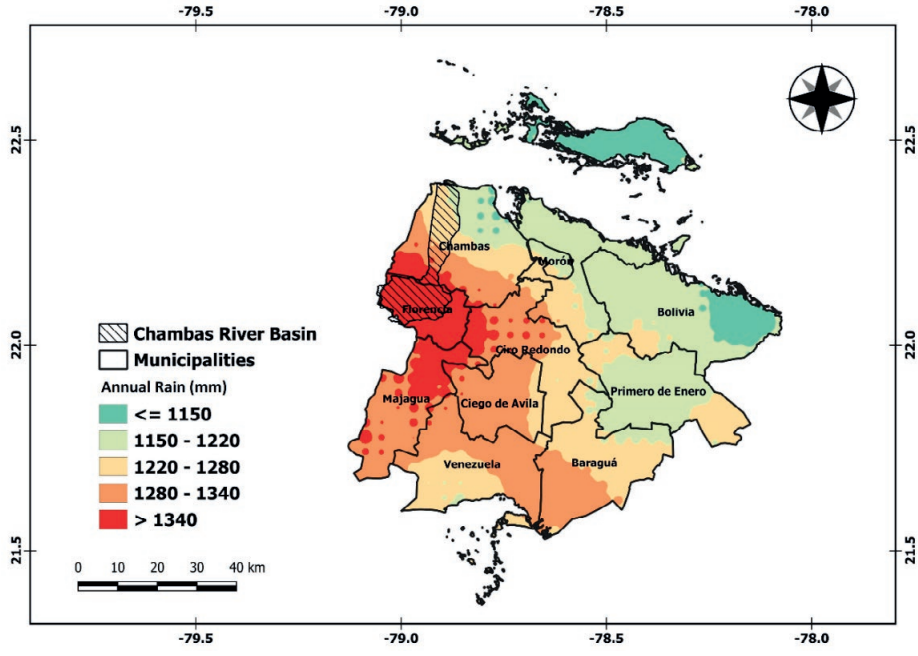

Figure 11. Spatial distribution of mean annual rain (mm) for Ciego de Ávila Province, central Cuba in the period 1961 – 2020.

Spatial distribution of annual rain in Ciego de Ávila Province showed that the Chambas River Basin is located in the areas with the greatest annual rain values (>1340 mm) in the province (western part), while the lowest annual rain values (<1150 mm) were recorded at the eastern part of the basin and in Cayo Coco island (Figure 5). Inside the basin, during the dry season, the highest rain values were recorded at the center (>310 mm) and the lowest to south (260–275 mm) (Figure 11). During the wet season, the highest rain values were found at the basin's south and center portions (1090 mm) and the lowest (950–970 mm) to the north of the basin.

3.2. Water area of reservoirs

Figures 12 and 13 show the water area of the reservoirs (between the wet season of 2014 and the dry season of 2021), calculated using the NDWI and images RADAR methods. We added

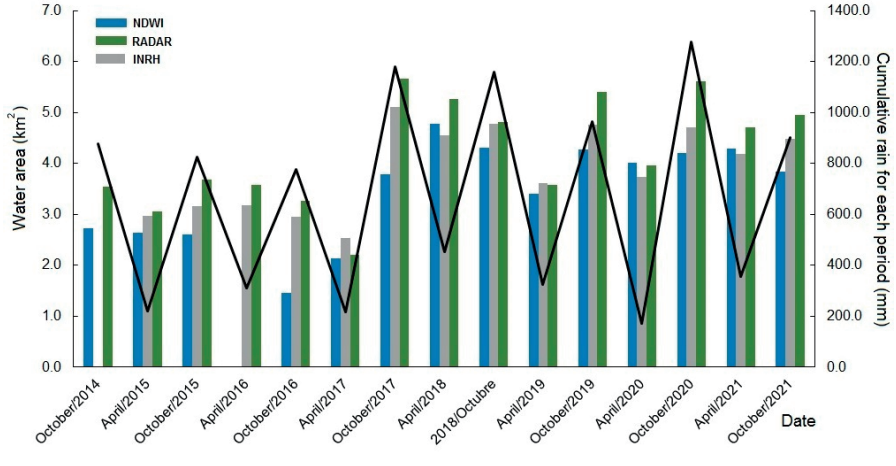

Figure 12. Water area (km^2) calculated by remote sensing methods and reported by the INRH in Cañada Blanca reservoir in the period 2014 – 2021. Black line represents the cumulative rain for each period (mm).

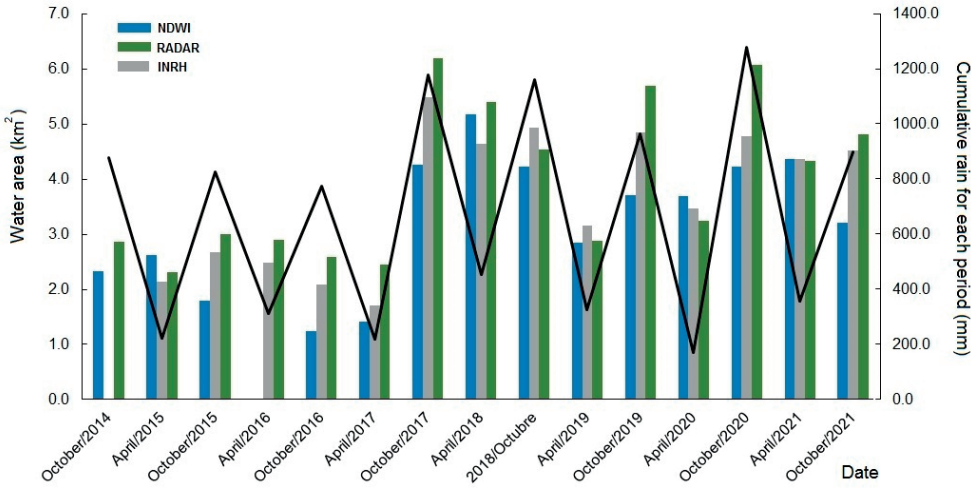

Figure 13. Water area (km^2) calculated by remote sensing methods and reported by INRH in Chambas II reservoir in the period 2014 – 2021. Black line represents the cumulative rain for each period (mm).

the water area (for the same studied period) of each reservoir reported by the National Hydraulic Resources Institute (INRH in Spanish) and the mean rain for each period to Figures 6 and 7. A Kruskal-Wallis non-parametric test did not show any significant differences between measured water areas using remote sensing methods (RSM) and the reported area using AVE curve. However, water areas measured with RSM were smaller (for both reservoirs) than the reported area measured with AVE curve. For both reservoirs, mean water areas measured with NDWI and RADAR were 19% and 8% smaller than the mean water area reported by authorities (INRH) for the same period.

Measured water areas of reservoirs varied seasonally, with a significant Spearman correlation (R=0.62 for Chambas II and R=0.61 for Cañada Blanca) with mean rain for each period inside the basin, only for water areas measured with RADAR images. In Chambas II reservoir, the greatest water area increases occurred (for both methods) from April to October of 2017 (2.8 km^2 using NDWI and 3.8 km^2 from RADAR method), while water area increase reported by authorities was 3.7 km^2. In Cañada Blanca reservoir, these increases were 1.6 km^2 using the NDWI and 2.6 km^2 using RADAR; INRH reported an increase of 3.5 km^2 of water area (Figures 14 and 15).

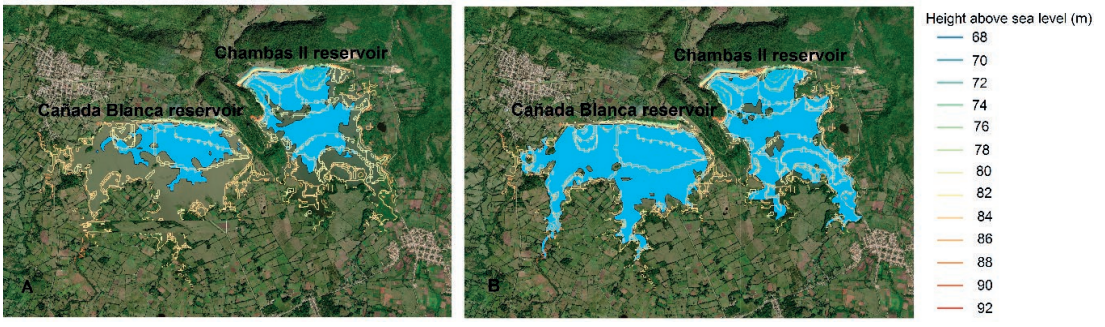

Figure 14. Water area variation in Cañada Blanca and Chambas II reservoirs between April (A) and October of 2017 (B) measured by NDWI method.

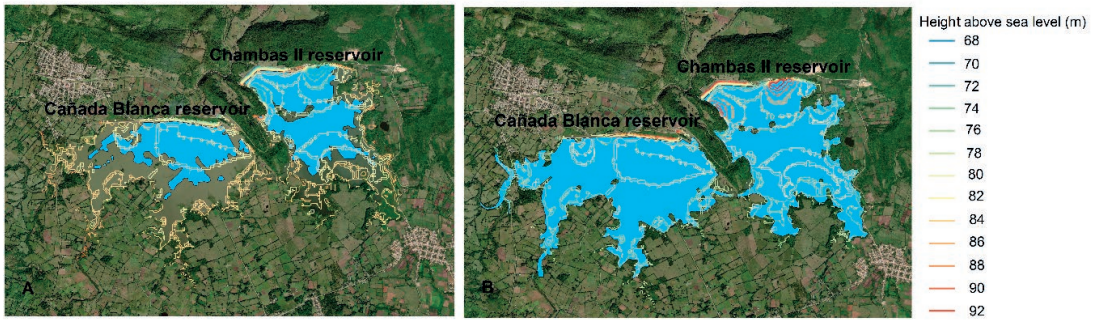

Figure 15. Water area variation in Cañada Blanca and Chambas II reservoirs between April (A) and October of 2017 (B) measured by RADAR method.

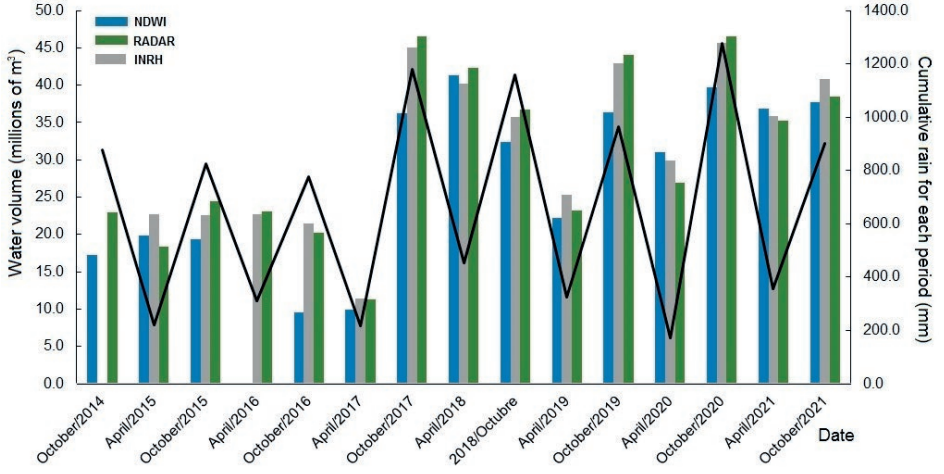

Figure 16. Water volume (millions of m^3) calculated by remote sensing methods and reported by the INRH in Cañada Blanca reservoir in the period 2014 – 2021. Black line represents the cumulative rain for each period (mm).

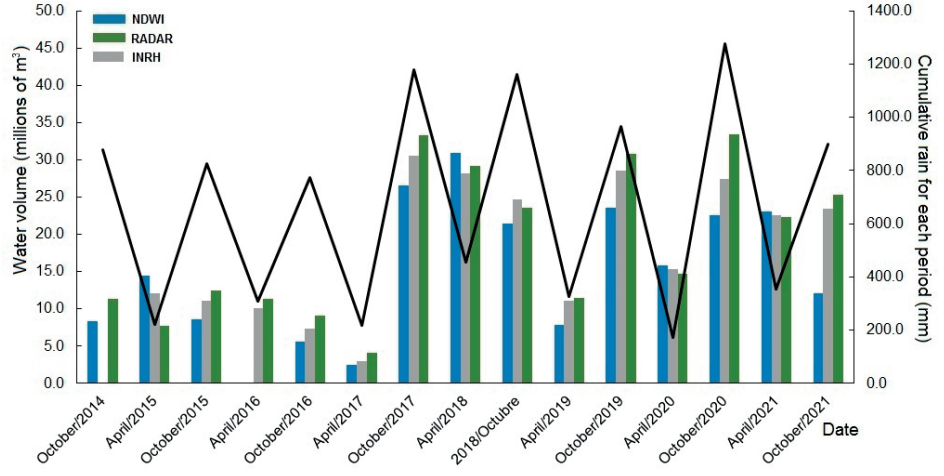

Figure 17. Water volume (millions of m^3) calculated by remote sensing methods and reported by INRH in Chambas II reservoir in the period 2014 – 2021. Black line represents the cumulative rain for each period (mm).

3.3. Water volume of reservoirs

The static water storage capacity (water volume) of both reservoirs varied (as area) between seasons with the greatest volume in both reservoirs recorded in October of 2017 (30.5 million of m^3 in Chambas II and 45.1 million of m^3 in Cañada Blanca reservoir) (Figures 16 and 17). A Kruskal-Wallis non-parametric test did not show any significant differences among measured water areas using both remote sensing methods (RSM) and reported area using AVE curve. In the case of water volume, the differences (not significant) among volumes were found in Chambas II, 15% lower with NDWI and 3% with RADAR methods than the volumes reported by the INRH (using AVE curve). For Cañada Blanca, water volume was 10% lower with NDWI but slightly higher with RADAR (2%). Both reservoirs did not show any significant correlation between volumes with the methods used nor with the use of rain or evaporation rates.

Similar to area, in both reservoirs, the greatest increase of water volume was documented from April to October of 2017 (between 23.0 and 27.0 million of m^3 in Chambas II and between 26.0 and 33.0 million of m^3 in Cañada Blanca) (Figures 10 and 11).

With the results obtained using remote sensing methods, empirical area – volume models were calculated for both reservoirs (Figure 18). These relations were calculated using a non-lineal regression method, as proposed by Lehner et al. (2011) for more than 5000 reservoirs around the world.

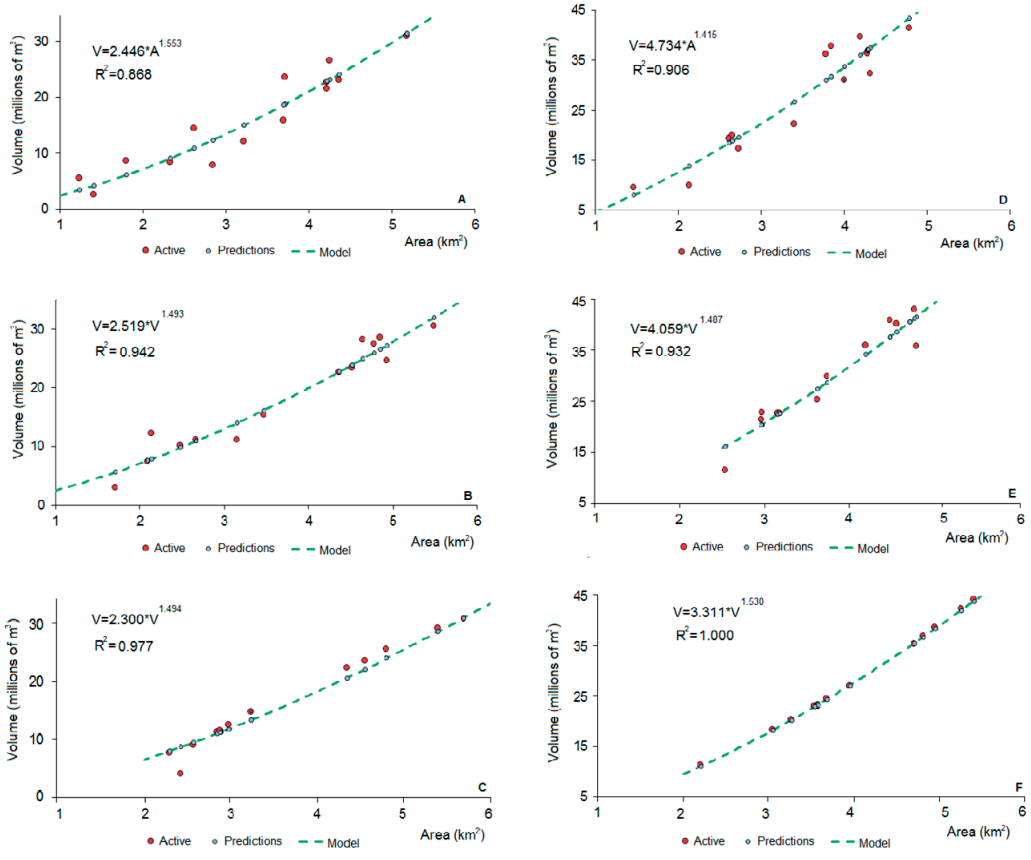

Figure 18. Non lineal regression Area vs Volume for Chambas II rerservoir for NDWI (A), RADAR (B), C (INRH) and Cañada Blanca reservoir for NDWI (D), RADAR (E) and INRH (F).

4. Discussion

This study is the first in Cuba directly related to water area and volume temporal variation using remote sensing methods in two water reservoirs.

Although remote sensing has been used as a new tool for monitoring water resources (Schwatke et al., 2019; Favoreto da Cunha et al., 2020; Nhat Quang et al., 2021) for some years, the use of these methods for water area and volume of reservoirs or lakes in Cuba is practically zero. Denis Ávila (2015) found the seasonal variation of vegetation cover associated with a water reservoir in eastern Cuba between 1978 and 2012 using Landsat images previously standardized and corrected; however, this research was different in objectives and results from our study.

The use of these RSM could help better management of water in reservoirs, particularly in developing countries like Cuba, where there are problems with management and operational processes (Rodrigues et al., 2012; Batista Silva et al., 2016; Nhat Quang et al., 2021). Also, as it could occur in Cuba and other countries, database of reservoirs are not available to other economic and social sectors (as the scientific community for example), so the possibility to use RSM tools are, taking into account our results, feasible for others sector not directly related with water management (Wang et al., 2013; Naba Sayl et., 2017).

The total water areas calculated with the use of RSM for each studied period were not significantly different from calculated areas using the AVE curve and reported by water managers. So, the results of this study are reliable in terms of accuracy in respect to data reported by authorities. This behavior was homogenous for both methods and reservoirs, respectively. Some studies found up to 87% of differences between water areas calculated by RSM and those reported by water managers (Wang et al., 2013), which did not occur in this study. Although RSM was reliable for water area calculation, RADAR methods proved to be better. The NDWI has some disadvantages when compared to the RADAR method. In fact, one of the disadvantages that was most evident in this study (differences between measured areas using NDWI and RADAR methods) resulted from the designed algorithm that was used for the NDWI processing method. All images used in this algorithm were coming of multiband images composed by diverse bands corresponding to satellite instruments based on solar light (Chuvieco, 2008); so, this implies that to obtain these images, it is necessary the abcense of clouds and enough solar light to observe land surface (passive teledetection) (Jin et al., 2007; Di Bella et al., 2008; Martínez et al., 2017). However, radar sensors obtain images using their own light spectra, which trough a reflextion process can work under any climatic condition (Polo, 2004), in a way that clouds can not damage image quality (active teledetection) (Martínez, 2005; Marchionni and Cavayas, 2014).

Over the study period (2014–2021), seasonal water area variation was highly dynamic (lower areas at end of the dry season and higher areas at end of the wet season) and in the case of RADAR methods, these variations were significant when correlated with mean annual rain for each period (Suleiman, 2014; Van Den Hoek et al., 2019**)**. The statistical analysis did not show any significant differences with evaporation rate; the other variable out of the analysis (we could not access this database) was water volumes extracted from the reservoir, which is a potential cause of water and volume seasonal variation. The greatest and most significant water area and volume variation (for both reservoirs) during the study period was from April to October of 2017, mainly due to the rain volume in the wet season of 2017 (1178.7 mm), although the accumulative rain for each period showed a higher volume in the wet season of October of 2020 (1277.8 mm). For both wet seasons (2017 and 2020), cumulative rain volumes had were influenced of two tropical cyclones (Hurricane Irma in September of 2017 and tropical storm Laura in August of 2020).

Like the water area, water volumes for each reservoir did not show any significant differences among water volumes measured using RSM and those reported by the authorities using AVE curve. The highest measured and reported water volumes (for both reservoirs) were at the end of the wet seasons of 2017 and 2020, coinciding with the greatest rain volumes for both periods (Haddeland et al., 2006; Döll et al., 2009; De Oliveira Xavier et al., 2020). The lowest water volume for the studied period was in April of 2017, caused by the low annual rain volume (896.4 mm) reported in 2016 (the lowest rain volume in the last decade).

Some studies (Lehner and Döll, 2004; Lehner et al., 2011; Van Bemmelen et al., 2016; Favoreto da Cunha et al., 2020) calculated area-volume models that are very useful to calculate stored water volumes using water areas measured through different methods as RSM. With our measured (by RSM) and reported areas (by authorities) of reservoirs, area – volume models using no – lineal regression methods were constructed. These models differed from the one proposed by Lehner et al. (2011), because these authors calculated the relation (area – volume for more than 5000 large reservoirs (more than 100 million m^3). However, calculated models for RMS and the calculated model for AVE curve (official measures reported by authorities) showed a good correlation (with R^2 greater than 88%). These results could be used as a tool to calculate stored water in reservoirs, using only the water areas measured by RSM (Rodrigues et al., 2012; Van Bemmelen et al., 2016; Favoreto da Cunha et al., 2020).

The present paper summarizes the seasonal water area and volume variations in two reservoirs using remote sensing methods and comparing the results with the values reported by local authorities (using AVE curve). These results show that RSM is a useful tool for monitoring water resources in Central Cuba, which could be extrapolated to the rest of the reservoirs (smalls and larges) of the country.

5. Conclusions

Cañada Blanca and Chambas II are two important water reservoirs that have been used for some economic and social activities of Ciego de Ávila province (Central Cuba). Remote sensing methods (using NDWI and RADAR images) were suitable means to obtain water area and volumes and their variations during the studied period. These results were consistent with those values reported by the INRH. Our results show that remote sensing methods are useful, acute and economic tools for monitoring of water surface in natural and artificial reservoirs, regardless of the advantages of RADAR method over NDWI method. The advantages of these methods are the low costs and reduction of the workload for post-data processing and it has shown its economic efficiency for reservoir management, so, that there would be possibilities to react appropriately in the decision making process. While, largest limitations are related with spatial resolution and clouds cover (in the case of NDWI) and the internet access (low speed of connection) in Cuba. Large deviations of water area and volumes occurred during the dry season (lower values) and the wet season of 2017 (influenced by rain associated to of Hurricane Irma) and wet season of 2020 (influenced by rain associated to tropical storm Laura).

Calculated area – volume models with significant statistical correlation are another useful tool that could be used to improve water management in terms of accuracy and to increase reliable results in cases where gauge measurements are scarce or not available.

References

Adediji, A., Ajibade, L.T. 2008. The change detection of major dams in Osun State, Nigeria using remote sensing (RS) and GIS techniques. *Journal of Geography and Regional Planning*, *1*(6), 110-115.

Aguilar, C., Zinnert, J.C., Polo, M.J., Young, D.R. 2012. NDVI as an indicator for changes in water availability to woody vegetation. *Ecological Indicators*, *23*, 290-300. https://doi.org/10.1016/j.ecolind.2012.04.008

Alarcón, D. 2021. Análisis de la disminución del cuerpo de agua de la laguna de Aculeo utilizando imágenes de radar de Sentinel -1A/1B y de Global Surface Water Explorer. *Revista Cartógrafo*, *1*(1), 5-14.

Batista Silva, J.L. 2016. Evaluación de los recursos hídricos de Cuba. *Revista Geográfica*, *157*, 73-83.

Chuvieco, E. 2008. *Teledetección ambiental, la observación de la Tierra desde el espacio*. 3ª edición. Editorial Ariel, Barcelona, España.

Cobos, M.E., Cruz, D.D., Hernández, M. 2016. Análisis multitemporal del Índice Normalizado de Diferencia de Vegetación (NDVI) en Cuba. *Revista del Jardín Botánico Nacional*, *37*, 15-18.

Cruz Flores, D.D., Curbelo Benítez, E.A., Ferrer-Sánchez, Y., Ávila, D.D. 2020. Variaciones espaciales y temporales en el Índice de Vegetación de Diferencia Normalizada en Cuba. *Ecosistemas*, *29*(1), 1885. https://doi.org/10.7818/ECOS.1885

Denis Ávila, D. 2015. Análisis multitemporal de imágenes Landsat para evaluar las variaciones de la cobertura vegetal emergente en la laguna Leonero, Granma, Cuba. *Revista del Jardín Botánico Nacional*, *36*, 47-53.

De Oliveira Xavier, G., de Almeida, T., Magno Moreira de Oliveira; C., Silva de Oliveira, P.D., Barros Costa; V.H., Moreira Alves Granado, L. 2020. Estimate and evaluation of reservoir metrics in Serra da Mesa dam (GO) using the Google Earth Engine platform. *Ambiente & Água - An Interdisciplinary Journal of Applied Science*, *15*(5), e2584. https://doi.org/10.4136/ambi-agua.2584

Di Bella, C.M., Posse, G., Beget, M.E., Fischer, M.A., Mari, N., Veron, S. 2008. La teledetección como herramienta para la prevención, seguimiento y evaluación de incendios e inundaciones. *Ecosistemas*, *17*(3), 39-52.

Döll, P., Fiedler, K., Zhang, J. 2009. Global-scale analysis of river flow alterations due to water withdrawals and reservoirs. *Hydrology and Earth System Sciences, 13*, 2413-2432. https://doi.org/10.5194/hess-13-2413-2009

Du, Z., Bin, L., Feng, L., Wenbo, L., Weidong, T., Hailei, W., Yuanmiao, G., Bingyu, S., Xiaoming, Z. 2012. Estimating surface water area changes using time-series Landsat data in the Qingjiang River Basin, China. *Journal of Applied Remote Sensing*, *6*, https://doi.org/10.1117/1.JRS.6.063609

Escobar-Flores, J.G., Sandoval, S., Valdez, R., Shahriary, E., Torres, J., Álvarez-Cárdenas, S., Gallina-Tessaro, P. 2019. Waterhole detection using a vegetation index in desert bighorn sheep (*Ovis Canadensis cremnobates*) habitat. *PLoS ONE*, *14*(1), e0211202. https://doi.org/10.1371/journal.pone.0211202.

Favoreto da Cunha, C., Brandão Cardoso, S., Hideo Teramoto, E., Kiang Chang, H. 2020. Modelo área-volume para a Represa Guarapiranga empregando o índice NDWI. *Holos Environment*, *20*(1), 137-151. https://doi.org/10.14295/holos.v20i1.12370

Fuentes, I., Padarian, J., van Ogtrop, F., Vervoort, R.W. 2019. Comparison of Surface Water Volume Estimation Methodologies That Couple Surface Reflectance Data and Digital Terrain Models. *Water*, *11*, 780. https://doi.org/10.3390/w11040780.

Haddeland, I., Skaugen, T., Lettenmaier, D.P. 2006. Anthropogenic impacts on continental surface water fluxes, *Geophysical Research Letters*, *33*, L08406. https://doi.org/10.1029/2006GL026047.

Hernández, M., Cruz, D. 2016. Cobertura de vegetación natural en Parques Nacionales de Cuba: análisis multitemporal y variación futura de las condiciones bioclimáticas. *Revista del Jardín Botánico Nacional*, *37*, 93-102.

Instituto Nacional de Recursos Hidráulicos (INRH). 2018. *Boletín Hidrológico*. Octubre 2018. Servicio Hidrológico y Disponibilidad. pp 16.

Jakovljevic, G., Govedarica, M., Álvarez-Taboada, F. 2018. Waterbody mapping: a comparison of remotely sensed and GIS open data sources, *International Journal of Remote Sensing, 40*(8), 2936-2964. https://doi.org/10.1080/01431161.2018.1538584

Jin, Y.Q., Yan, F. 2007. A change detection algorithm for terrain surface moisture mapping based on multi-year passive microwave remote sensing (Examples of SSM/I and TMI Channels). *Hydrological Processes*, *21*, 1918-1924. https://doi.org/10.1002/hyp.6401

Karran, D.J., Westbrook, C.J., Wheaton, J.M., Johnston, C.A., Bedard-Haughn, A. 2016. Rapid surface water volume estimations in beaver ponds. *Hydrology and Earth System Sciences Discuss.*, *352*, 1-26. https://doi.org/10.5194/hess-2016-352.

Kendall, M. 1975. *Multivariate Analysis*. Charles Griffin & Company, London.

Lee, J.S. 1980. Digital Image Enhancement and Noise Filtering by use of Local Statistics. *IEE Transactions on Pattern Analysis and Machine Intelligence*, *2*, 165-168. https://doi.org/10.1109/TPAMI.1980.4766994

Lee, J.S. 1981a. Refined Filtering of Image Noise Using Local Statistics. *Computer Graphics and Image Processing*, *15*(4), 380-389. https://doi.org/10.1016/S0146-664X(81)80018-4

Lee, J.S. 1981b. Speckle Analysis and Smoothing of Synthetic Aperture Radar Images. *Computer Graphics and Image Processing*, *17*(1), 24-32. https://doi.org/10.1016/S0146-664X(81)80005-6

Lehner, B., Döll, P. 2004. Development and validation of a global database of lakes, reservoirs and wetlands. *Journal of Hydrology*, *296*(1-4), 1-22. https://doi.org/10.1016/j.jhydrol.2004.03.028

Lehner, B., Liermann, C.R., Revenga, C., Vörösmarty, C., Fekete, B., Crouzet, P., Döll, P., Endejan, M., Frenken, K., Magome, J., Nilsson, C., Robertson, J.C., Rödel, R., Sindorf, N., Wisser, D. 2011. *Global reservoir and dam database.* Version 1.1 (GRanDv1): Dams, Revision 01. Palisades, NY: NASA Socioeconomic Data and Applications Center (SEDAC). pp. 12.

Lopes, F.B., Barbosa, C.C., Novo, E M., Andrade, E.M.D., Chaves, L.C. 2014. Modelagem da qualidade das águas a partir de sensoriamento remoto hiperespectral. *Revista Brasileira de Engenharia Agrícola e Ambiental*, *18*, 13-19. https://doi.org/10.1590/1807-1929/agriambi.v18nsupps13-s19

Machado, M.T. de S.; Baptista, G.M. de M. 2016. Sensoriamento remoto como ferramenta de monitoramento da qualidade da água do Lago Paranoá (DF). *Engenharia Sanitária e Ambiental*, *21*(2), 357-365. http://doi.org/10.1590/s1413-41522016141970

Mann H.B. 1945. Nonparametric tests against trend. *Econometrica*, *13*, 245-259. https://doi.org/10.2307/1907187

Marchionni, D.S., Cavayas, F. 2014. La Teledetección por Radar como fuente de Información Litológica Y Estructural. Análisis Espacial de Imágenes SAR de Radarsat-1, *GEOACTA*, *39*(1), 62-89.

Martínez, J. 2005. *Percepción Remota "Fundamentos de Teledetección Espacial"*. Comisión Nacional del Agua, CNA. México.

Martínez, M., Martínez, M.E., Martínez, E., Renza, D. 2017. Detection of Changes in Natural Aquifer Reservoirs based on the Index of Drought. *IEEE Latin America Transactions*, *15*(11), 2059-2063. https://doi.org/10.1109/TLA.2017.8070408

McFeeter, S.K. 1996. The use of the normalized difference water index (NDWI) in the delineation of open water features. *International Journal of Remote Sensing*, *17*, 1425-1432. https://doi.org/10.1080/01431169608948714

Morejón, M., Vega, M., Escarré, A., Gómez, R., Febles, J.M. 2010. Clasificación de la vegetación en los sectores superiores de cuencas de la región occidental de Pinar del Rio utilizando la teledetección. *Ciencias de la Tierra y el Espacio*, *11*, 60-68.

Mulligan, M., van Soesbergen, A., Sáenz, L. 2020. GOODD, a global dataset of more than 38000 georeferenced dams. *Scientific Data*, *7*, 31. https://doi.org/10.1038/s41597-020-0362-5

Muro, J., Strauch, A., Fitoka, E., Tompoulidou, M., Thonfeld, F. 2019. Mapping wetland dynamics with SAR-based change detection in the cloud. *Geoscience and Remote Sensing Letters IEEE*, 1-4. https://doi.org/10.1109/LGRS.2019.2903596

Muro, J., Varea, A., Strauch, A., Guelmami, A., Fitoka, E., Thonfeld, F. 2020. Multitemporal optical and radar metrics for wetland mapping at national level in Albania. *Heliyon*, *6*(8), e04496. https://doi.org/10.1016/j.heliyon.2020.e04496

Naba Sayl, K., Muhammad, N.S., El-Shafie, A. 2017. Optimization of area–volume–elevation curve using GIS–SRTM method for rainwater harvesting in arid areas. *Environmental Earth Sciences*, *76*, 368. https://doi.org/10.1007/s12665-017-6699-1

Nandi, D., Chowdhury, R., Mohapatra, J., Mohanta, K., Ray, D. 2018. Automatic Delineation of Water Bodies Using Multiple Spectral Indices. *International Journal of Scientific Research in Science, Engineering and Technology*, *4*(4), 498-512.

Nhat Quang, D., Khanh, L.N., Tam, H.S., Trung Viet, N. 2021. Remote sensing applications for reservoir water level monitoring, sustainable water surface management, and environmental risks in Quang Nam province, Vietnam. *Journal of Water and Climate Change*, *12*(7), 3045. https://doi.org/10.2166/wcc.2021.347

Park, J.W., Korosov, A., Babiker, M., Sandven, S., Won, J.S. 2018. Efficient Thermal Noise Removal for Sentinel -1 TOPSAR Cross-Polarization Channel. *IEEE Transactions on Geoscience and Remote Sensing*, *56*(3), 24-41. https://doi.org/10.1109/TGRS.2017.2765248

Pohlert,T. 2016. *Non-parametric Trend Tests and Change-Point Detection*. CC BY-ND, 4.

Ponvert-Delisles, B. 2016. Algunas consideraciones sobre el comportamiento de la sequía agrícola en la agricultura de Cuba y el uso de imágenes por satélites en su evaluación. *Revista Cultivos Tropicales*, *37*(3), 22-41.

Polo, P.L. 2004. Aplicaciones de imágenes de radar, en la generación de información para la mitigación de riesgos naturales. *Dialogo Andino*, *23*, 36-43

Rodrigues, L.N., Sano, E.E., Steenhuis, T.S., Passo, D.P. 2012. Estimation of small reservoir storage capacities with remote sensing in the Brazilian Savannah region. *Water Resources Management*, *26*, 873-882. https://doi.org/10.1007/s11269-011-9941-8

Rouse, J.W., Haas, R.H., Schell, J.A., Deering, D.W. 1973. Monitoring Vegetation Systems in the Great Plains with ERTS (Earth Resources Technology Satellite). In *Proceedings of Third Earth Resources Technology Satellite Symposium*, Greenbelt, ON, Canada, 10–14 December 1973; Volume SP-351, pp. 309–317.

Schwatke, C., Scherer, D., Dettmering, D. 2019. Automated Extraction of Consistent Time-Variable Water Surfaces of Lakes and Reservoirs Based on Landsat and Sentinel-2. *Remote Sens*ing, *11*, 1010. https://doi.org/10.3390/rs11091010

Suleiman, Y.M. 2014. The role of rain variability in reservoir storage management at Shiroro Hydropower Dam, Nigeria. AFRREV STECH. *An International Journal of Science and Technology*, *3*(2), 18-30. https://doi.org/10.4314/stech.v3i2.2

Valero, A., Matos-Pupo, F., Hernández, S. 2021. Uso de Dashboard y SIG en servicios climáticos de Ciego de Ávila: Nueva propuesta metodológica. *Universidad&Ciencia*, *10*(2), 196-211.

Van Bemmelen, C.W.T., Mann, M., De Ridder, M.P., Rutten, M.M., Van De Giesen, N.C. 2016. Determining water reservoir characteristics with global elevation data. *Geophysical Research Letters*, *43*(21), 11-278. https://doi.org/10.1002/2016GL069816

Van Den Hoek, J., Getirana, A., Chul Jung, H., Modurodoluwa A., Okeowo, M., Hyongki L. 2019. Monitoring Reservoir Drought Dynamics with Landsat and Radar/Lidar Altimetry Time Series in Persistently Cloudy Eastern Brazil. *Remote Sensing*, *11*, 827. https://doi.org/10.3390/rs11070827

Xu, H. 2006 Modification of normalized difference water index (NDWI) to enhance open water features in remotely sensed imagery. *International Journal of Remote Sensing*, *27*, 3025-3033. https://doi.org/10.1080/01431160600589179

Wang, X., Yan, Ch. Song, L., Chen, X., Xie, H., Liu, L. 2013. Analysis of lengths, water areas and volumes of the Three Gorges Reservoir at different water levels using Landsat images and SRTM DEM data. *Quaternary International*, *304*, 115-125. https://doi.org/10.1016/j.quaint.2013.03.041

Wilson, E.H., Sader, S.A. 2002. Detection of forest harvest type using multiple dates of Landsat TM imagery. *Remote Sensing Environment*, *80*, 385-396. https://doi.org/10.1016/S0034-4257(01)00318-2